Applied Catalysis B: Environmental 123–124 (2012) 78–83

Contents lists available at SciVerse ScienceDirect

Applied Catalysis B: Environmental

journal homepage: www.elsevier.com/locate/apcatb

Nanocrystalline pyrochlore $AgSbO_3$: Hydrothermal synthesis, photocatalytic activity and self-stable mechanism study

Wenjun Liu, Xiaobin Liu, Yanghe Fu, Qingqing You, Renkun Huang, Ping Liu, Zhaohui Li*

Research Institute of Photocatalysis, Fujian Provincial Key Laboratory of Photocatalysis–State Key Laboratory Breeding Base, Fuzhou University, Fuzhou 350002, PR China

ARTICLE INFO

Article history:
Received 25 November 2011
Received in revised form 16 April 2012
Accepted 22 April 2012
Available online 27 April 2012

Keywords:
Hydrothermal
Pyrochlore $AgSbO_3$
Photocatalytic
Visible light
Self-stable mechanism

ABSTRACT

Nanocrystalline pyrochlore $AgSbO_3$ has been successfully synthesized by a facile hydrothermal method and was fully characterized by X-ray diffraction (XRD), UV–vis diffuse reflectance spectroscopy (DRS), scanning electron microscopy (SEM) and X-ray photoelectron spectroscopy (XPS). The as-prepared pyrochlore $AgSbO_3$ showed a higher photocatalytic activity in the degradation of typical dye as compared to that prepared by the solid-state reaction. The photocatalytic mechanism of pyrochlore $AgSbO_3$ and its stability during photocatalytic reactions was investigated. It was found that pyrochlore $AgSbO_3$ can maintain its structure stability and photocatalytic activity under visible light irradiations by partial formation of metallic Ag and Ag_2O on its surface during the photocatalytic degradation of organic pollutants. This study provides some new insights into the photocatalytic mechanism of Ag-based multi-metal oxide photocatalysts.

1. Introduction

Semiconductor-based photocatalytic oxidation has been established to be one of the most promising technologies for the environment remediation and has been employed in the treatment of all kinds of organic contaminants [1–3]. However, with a relatively wide band gap (3.2 eV), the commonly used photocatalyst TiO_2 can only absorb a small fraction of solar energy and thus restrict its practical applications. The effective application of photocatalysis in environmental remediation requires that the photocatalysts should be highly efficient under visible light. During the past decade, tremendous effort has been devoted to the development of new photocatalysts capable of operating in the visible light region. In addition to metal and non-metal ions doped TiO_2, single-phase multi-metal oxides, metal sulfides, silver orthophosphate and halides have been demonstrated to be efficient photocatalytic materials under visible light irradiations [4–11].

Ag-containing complex oxides are promising visible light sensitive photocatalysts. In these Ag-based complex oxides, the tops of their valence band (VB) are usually comprised of hybridized Ag 4d and O 2p orbitals. Such hybridization can induces a shift of the top of VB to a higher energy and make the band-gap narrower. Several Ag-containing complex oxides like $AgNbO_3$, Ag_3VO_4 and $AgSbO_3$ have already been reported to be visible light responsive photocatalysts [12–14]. Among them, cubic pyrochlore $AgSbO_3$ prepared via a solid state reaction has been revealed to decompose water to produce O_2 in the presence of silver nitrate and to decompose gaseous propanol under visible light irradiations.[12] The structure of the cubic pyrochlore $AgSbO_3$ is constructed by the combination of AgO_6 and SbO_6 octahedra, in which a network of the corner-sharing SbO_6 octahedra forms a parallel hexagonal-prism channel along the (1 1 1) direction. A later study by Singh and Uma revealed that the photocatalytic activity of the cubic pyrochlore $AgSbO_3$ is sensitive to the amount of silver and might change drastically even to a small variation in silver amount [15]. However the already reported method in the preparation of pyrochlore $AgSbO_3$ is the conventional solid-state reaction. In the solid-state reaction, it is difficult to control the reaction condition to have stoichiometric pyrochlore $AgSbO_3$ since the partial volatilization of Ag during the high temperature calcination is usually unavoidable. Besides this, it is generally known that products obtained via the solid-state process usually contain undesirable phase and is inhomogeneous due to the high temperature sintering process. Soft chemical methods like hydrothermal/solvothermal method have been demonstrated to be effective methods in the preparations of nanocrystalline metal oxides with large specific surface area. Our previous study has indicated that nanocrystalline antimonates with high specific surface area can be prepared from Sb_2O_5 via a facile hydrothermal method [16,17]. It would be interesting to see whether such a facile hydrothermal method can be applied to the preparation Ag-containing antimonates like $AgSbO_3$.

In this study, we reported the successful synthesis of nanocrystalline pyrochlore $AgSbO_3$ via a facile hydrothermal method and its photocatalytic activity for the degradation of a typical dye RhB.

* Corresponding author. Tel.: +86 591 83779260; fax: +86 591 83779105.
E-mail address: zhaohuili1969@yahoo.com (Z. Li).

0926-3373/$ – see front matter © 2012 Elsevier B.V. All rights reserved.
http://dx.doi.org/10.1016/j.apcatb.2012.04.033

The photocatalytic mechanism of pyrochlore $AgSbO_3$, especially its interesting self-stable mechanism during the photocatalytic reaction is also revealed.

2. Experimental

2.1. Syntheses

All of the reagents were analytical grade and used without further purifications. Nanocrystalline pyrochlore $AgSbO_3$ samples were prepared by a hydrothermal method. In a typical procedure, Sb_2O_5 powder (0.24 g, 0.75 mmol) was added to 70 ml aqueous solution containing AgAc (0.25 g, 1.5 mmol) under vigorous stirring. The pH of the resulting mixture was adjusted by nitric acid solution or sodium hydrate solution. The mixture was loaded into a 100 mL Teflon-lined autoclave and sealed tightly. The autoclaves were kept at 180 °C for 48 h. After cooling to room temperature, the precipitate was collected, washed with distilled water and absolute ethanol for several times, and then dried in air at 80 °C. For comparison, bulk pyrochlore $AgSbO_3$ sample was prepared from Ag_2O and Sb_2O_5 via the conventional solid-state reaction according to the literature.

2.2. Characterizations

X-ray diffraction (XRD) patterns were collected on a Bruker D8 Advance X-ray diffractometer with Cu Kα radiation. The accelerating voltage and the applied current were 40 KV and 40 mA, respectively. Data were recorded at a scanning rate of $0.004^\circ\ 2\theta\ s^{-1}$ in the 2θ range of 10–70°. UV–vis absorption spectrum (UV–vis DRS) of the product was obtained for the dry-pressed disk samples using a UV–vis spectrophotometer (Cary 500 Scan Spectrophotometers, Varian, USA). $BaSO_4$ was used as a reflectance standard in the UV–vis diffuse reflectance experiment. Morphology of the sample was characterized by field emission scanning electron microscopy (SEM) (JSM-6700F). X-ray photoelectron spectroscopy (XPS) measurement was performed on a PHI Quantum2000 XPS system with a monochromatic Al Kα source and a charge neutralizer. The binding energies were referred to the C 1s peak at 284.8 eV of the surface adventitious carbon. The total organic carbon concentration (TOC) was conducted in Shimadzu TOC-V (CPH) total carbon analyzer.

2.3. Photocatalytic activity measurements

The photocatalytic activity of the as-prepared pyrochlore $AgSbO_3$ evaluated by photocatalytic decomposition of RhB in an aqueous solution under visible light irradiations as a model reaction. 80 mg of the photocatalyst was added to 80 mL of RhB solution (10^{-5} mol/L). A 500 W tungsten halogen lamp was positioned inside a cylindrical Pyrex vessel and surrounded by a circulating water jacket (Pyrex) to cool the lamp. A cutoff filter was placed outside the Pyrex jacket to completely remove all wavelengths less than 420 nm to ensure the irradiation with visible light only. Prior to irradiations, the suspension was magnetically stirred in the dark for ca. 4 h to ensure the establishment of an adsorption/desorption equilibrium. At given irradiation time intervals, 4 mL of the suspensions were collected, centrifuged, and filtered through a Millipore filter to separate the photocatalyst particles. The degraded solutions of RhB were analyzed by a Varian Cary 500 Scan UV–vis spectrophotometer and the absorption peak at 554 nm for RhB was monitored. The percentage of degradation is reported as C/C_0. C is the absorption of RhB at each irradiated time interval of the maximum peak of the absorption spectrum at wavelength 554 nm. C_0 is the absorption of the starting concentration when adsorption/desorption equilibrium was achieved.

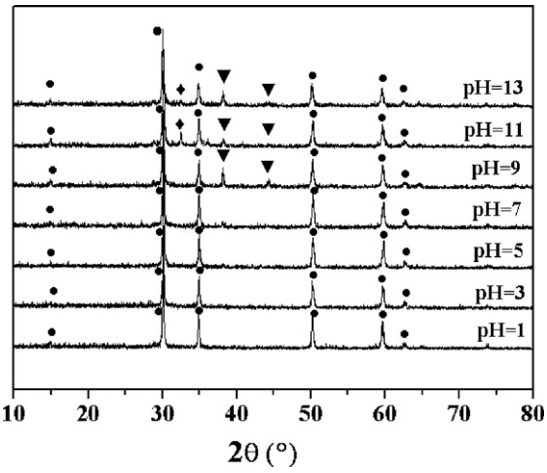

Fig. 1. XRD patterns of the resultant products through the hydrothermal process at 180 °C for 48 h under different pH values. (●) pyrochlore $AgSbO_3$; (▼) Ag; (♦) Ag_2O.

3. Results and discussion

In the reactions between Sb_2O_5 and AgAc, the pH value played an important role in controlling the composition of the final products. Fig. 1 shows the XRD patterns of the resultant products through the hydrothermal process at 180 °C for 48 h under different pH values. For pH value ranged from 1 to 7, the resultant product was pure pyrochlore $AgSbO_3$. When pH value was increased to 9, Ag was also obtained in addition to pyrochlore $AgSbO_3$. When the pH value was increased to 11, a mixture of pyrochlore $AgSbO_3$, Ag and Ag_2O was obtained. The XRD result is consistent with the observations that the color of the products changed from yellow to dark grey when the pH value in the reaction system increased.

The XPS spectrum in the Ag 3d region for the product obtained at pH of 5 is shown in Fig. 2a. Characteristic binding energy (BE) values of 367.4 eV for Ag $3d_{5/2}$ and 373.5 eV for Ag $3d_{3/2}$ are observed and indicate that Ag exists as Ag^+ in the product [18,19]. The SEM image shows that the as-prepared product consists of particles in the size of around 100 nm (Fig. 2b). However, the sample is sensitive to the electron beam and small fibers grow on the surface of the original particles during the SEM imaging process (Fig. 2c). UV–vis DRS of the as-prepared sample was measured and the result was shown in Fig. 2d. The wavelength at the absorption edge, λ, is determined as the intercept on the wavelength axis for a tangent line drawn on the absorption spectra. By applying this method, the absorption edge for the as-prepared pyrochlore $AgSbO_3$ can be determined to be ca. 472 nm, corresponding to a band gap of 2.6 eV. This value is consistent with that reported previously [14].

The photocatalytic activity of the as-prepared pyrochlore $AgSbO_3$ was evaluated by the degradation of RhB under visible-light irradiations. The temporal evolution of the spectral changes and the RhB concentration change as monitored by the maximum absorption of RhB at 554 nm during the photodegradation of RhB over hydrothermally prepared pyrochlore $AgSbO_3$ is shown in Fig. 3a and b respectively. As shown in Fig. 3a, the decrease of the intensity of the main peak of RhB at 554 nm was accompanied by a concurrent gradual hypsochromic shift of the main peak to a shorter wavelength during the visible light irradiations. This gradual hypsochromic shift has been well established to be a step-by-step de-ethylation of RhB, while the decrease of the intensity indicates the cleavage of the whole conjugated chromophore structure of RhB [20]. This observation indicates that the photocatalytic degradation

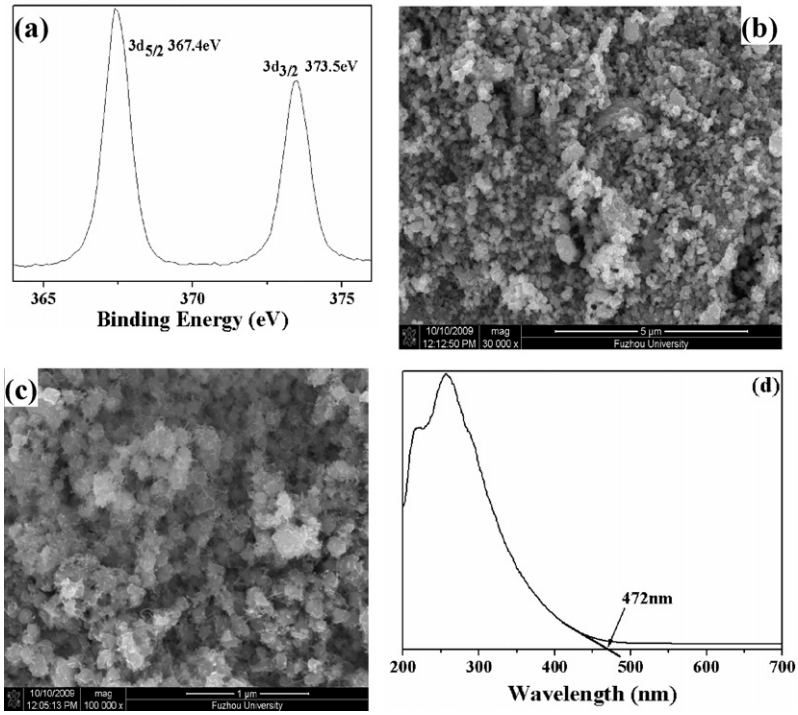

Fig. 2. Product obtained at pH 5 (a) XPS spectrum at Ag 3d region; (b) SEM image; (c) SEM image after prolong SEM image process; (d) UV–vis DRS.

of RhB over the irradiated pyrochlore $AgSbO_3$ proceeds via a simultaneous de-ethylation and the chromophore cleavage pathways. As shown in Fig. 3a, all RhB can be converted within 5 h and after irradiated for a total of 6.5 h, all the peaks corresponding to RhB or its derivatives disappeared, indicating that RhB has totally been decomposed to small organics or CO_2. The TOC changed from the original 149.04 mg/L to 2.6 mg/L after 6.5 irradiations, further confirming that almost all RhB has been mineralized. On the contrary, over pyrochlore $AgSbO_3$ prepared by a solid state reaction, 56% of RhB was converted in 6 h irradiations and even after irradiated for 13 h, only 93% RhB has been converted (Fig. 3b). It is obvious that the hydrothermally prepared pyrochlore $AgSbO_3$ shows a superior photocatalytic performance than that prepared via the convention solid-state reaction.

The stability of the photocatalyst is important for its application. To study the stability of pyrochlore $AgSbO_3$ as a photocatalyst, after the photocatalytic reaction, $AgSbO_3$ was centrifuged, filtered and was added to fresh RhB solution for a repeated use. The spectral changes and the RhB concentration change during the photocatalytic degradation of RhB over the second time used $AgSbO_3$ are shown in Fig. 4a and b respectively. To our surprise, we found that after the first photocatalytic reaction, used $AgSbO_3$ showed a higher photocatalytic activity for the degradation of RhB in the second time use. Only within 1 h, the main peak at 554 nm which corresponds to RhB shifted to 497 nm, indicating that all RhB had been converted to the de-ethylated product rhodamine. After irradiated for another 3 h, the peak at 497 nm totally disappeared and indicated that all rhodamine had been decomposed to small molecules or CO_2. The total time required for a complete decomposition of RhB over used $AgSbO_3$ was 4 h, much shorter than that (6.5 h) required for a complete decomposition over fresh hydrothermally prepared $AgSbO_3$. This observation is quite unexpected since usually fresh catalysts exhibit superior performance than the used one. The photocatalytic degradation of RhB over the hydrothermally prepared pyrochlore $AgSbO_3$ had been repeated for five times and the RhB concentration change as monitored by the maximum absorption of

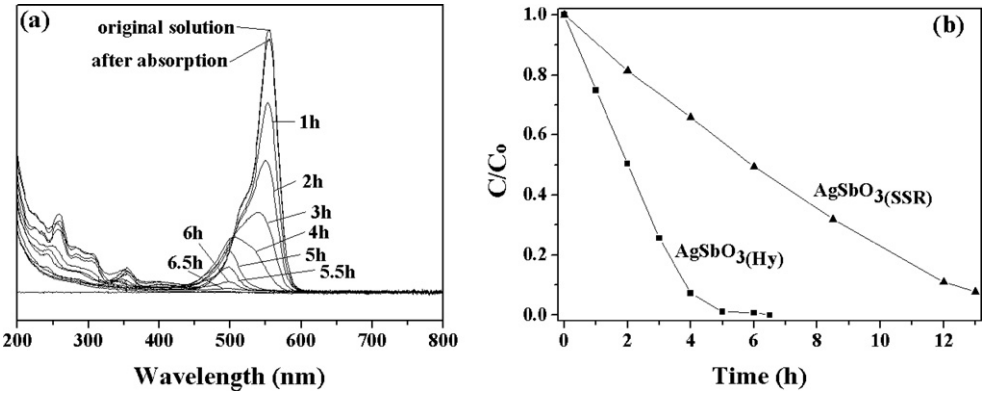

Fig. 3. (a) Temporal absorption spectral patterns of RhB during the photodegradation process over hydrothermally prepared pyrochlore $AgSbO_3$ (first run); (b) Temporal change of RhB concentration as monitored by the UV–vis absorption spectra at 554 nm over pyrochlore $AgSbO_3$ prepared via the hydrothermal method and solid state reaction (first run).

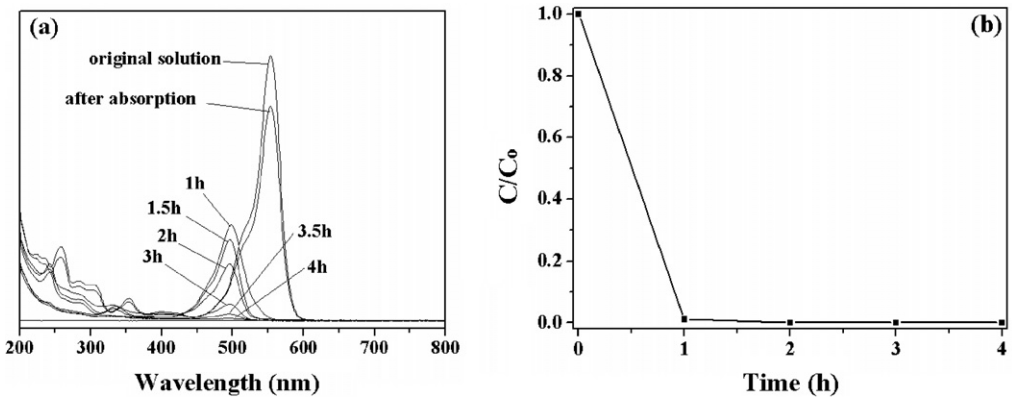

Fig. 4. (a) Temporal absorption spectral patterns of RhB during the photodegradation process over hydrothermally prepared pyrochlore $AgSbO_3$ (second run); (b) Temporal change of RhB concentration as monitored by the UV–vis absorption spectra at 554 nm over hydrothermally prepared pyrochlore $AgSbO_3$ (second run).

RhB at 554 nm during the photodegradation of RhB for all 5 runs are compared in Fig. 5. Although pyrochlore $AgSbO_3$ in the second use showed a remarkable enhanced photocatalytic activity, there was no much change in the photocatalytic performance of $AgSbO_3$ in the following 3 runs and implies that after the second run, the catalyst remains stable during the following several photocatalytic reactions.

The significant difference in the performance of the photocatalyst between the first and the second run implies that the composition or the structure of the photocatalyst may have changed after the first run. To elucidate this, characterizations were carried out on $AgSbO_3$ after the first run and the UV–vis DRS and XRD of used $AgSbO_3$ were shown in Figs. 6 and 7 respectively. It is found that the UV–vis DRS of $AgSbO_3$ after the first run showed a small absorption at ca. 520 nm as well as an enhanced absorption in the whole visible light region. The absorption at ca. 520 nm can be ascribed to the plasmonic resonance of Ag nanoparticles while the absorption in the whole visible light region can be attributed to Ag_2O. The existence of Ag and Ag_2O has also been confirmed by the XRD of $AgSbO_3$ after the first run by showing the peaks at 2θ of 38.1° and 44.3°, which corresponds to (1 1 1) and (2 0 0) plane of Ag, and the peak at 2θ of 32.8° corresponds to the (1 1 1) plane of Ag_2O. These observations indicate that after the first photocatalytic reaction, Ag and Ag_2O deposit on the surface of $AgSbO_3$. It is the co-existence of Ag and Ag_2O that is responsible for the enhancement of the photocatalytic performance of pyrochlore $AgSbO_3$ in the second run since Ag_2O–Ag composite itself has previously been revealed to be a highly active visible-light photocatalyst [21]. However the as-formed $AgSbO_3$–Ag–Ag_2O composite can maintain its stability during the following next 3 runs as evidenced from the stable photocatalytic performance (Fig. 5) and the unchanged XRD and UV–vis DRS of the photocatalyst after the following photocatalytic reactions. Although the in situ formed Ag and Ag_2O significantly improve the photocatalytic performance of $AgSbO_3$, the studies on the photocatalytic performance of directly deposited Ag/$AgSbO_3$,

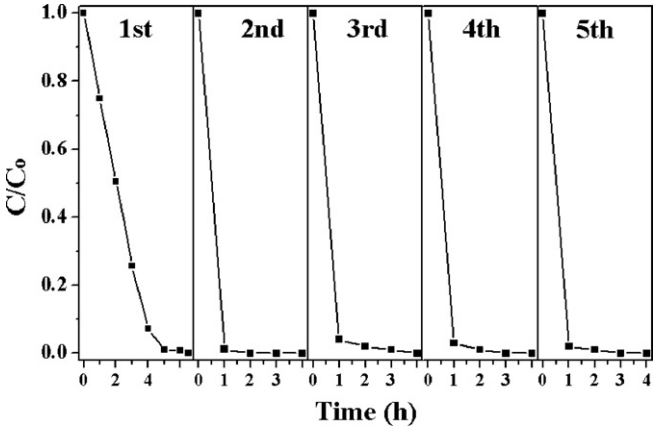

Fig. 5. Cycling runs in the photocatalytic degradation of RhB in the presence of hydrothermally prepared pyrochlore $AgSbO_3$ under visible-light irradiations.

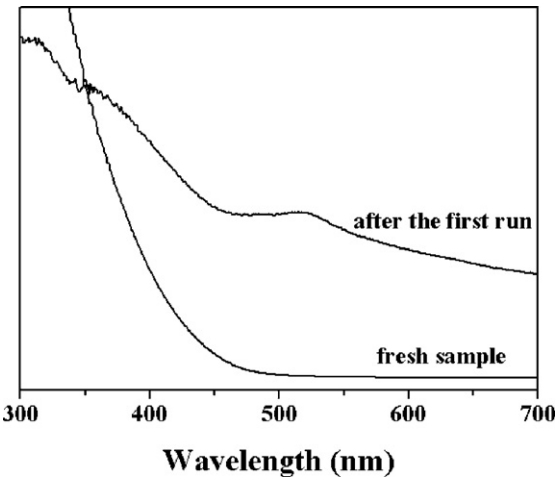

Fig. 6. UV–vis DRS of hydrothermally prepared pyrochlore $AgSbO_3$ after the first run.

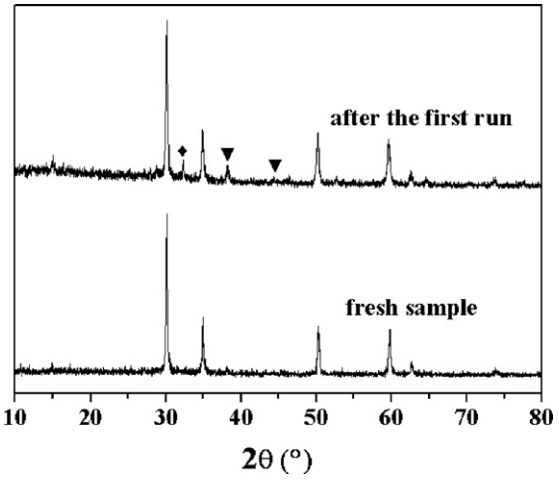

Fig. 7. XRD patterns of hydrothermally prepared pyrochlore $AgSbO_3$ after the first run. (▼) Ag; (♦) Ag_2O.

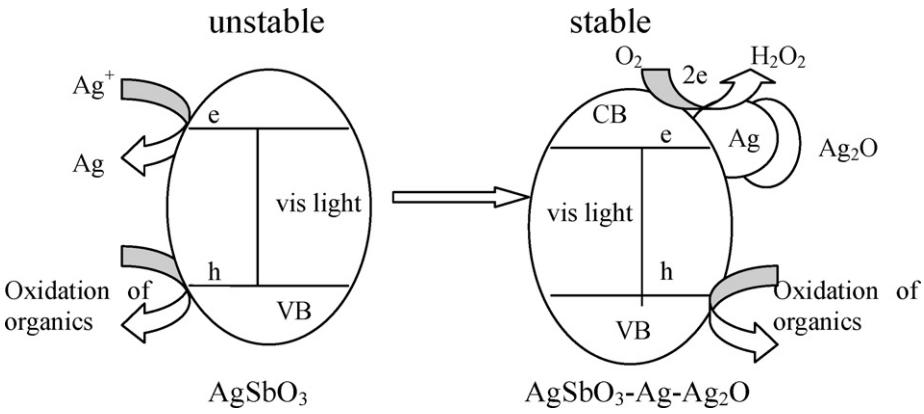

Scheme 1. The schematic diagram showing the photocatalytic mechanism of pyrochlore $AgSbO_3$ during the photocatalytic reaction.

$Ag_2O/AgSbO_3$ and $Ag–Ag_2O/AgSbO_3$ indicate not only the concentration of Ag and Ag_2O, but also their existing state influence the photocatalytic performance of $Ag–Ag_2O/AgSbO_3$ composites (Supporting materials Figs. S1–S3). Therefore it is believed that the enhanced photocatalytic performance observed over the second time used $AgSbO_3$ may be due to the unique in situ formed $AgSbO_3–Ag–Ag_2O$ structure.

The photocatalytic mechanism as well as the self-stable mechanism of pyrochlore $AgSbO_3$ during the photocatalytic reactions can be proposed as following. When pyrochlore $AgSbO_3$ is irradiated with visible light, photo-generated electrons are produced in the conduction band while photo-generated holes remain in the valence band of pyrochlore $AgSbO_3$. In the beginning, the photo-generated electrons preferably transfer to the lattice Ag^+ and reduce Ag^+ to form Ag nanoparticles on the surface of $AgSbO_3$ since Ag^+/Ag possesses a more positive potential (0.7991 V vs NHE) as compared to that of $O_2/HO_2^\bullet$ (−0.046 V vs NHE) [22]. The as-formed Ag nanoparticles can react further with O_2 to give Ag_2O on its surface and thus $AgSbO_3–Ag–Ag_2O$ composite is formed. The formation of Ag and Ag_2O in pyrochlore $AgSbO_3$ after the first photocatalytic reaction is evidenced from the XRD and UV–vis DRS. However, once a certain amount of metallic Ag is formed on the surface of pyrochlore $AgSbO_3$, the metallic Ag sites can act as an electron pool and transfers the photo-generated electrons to oxygen through multi-electron transfer routes. Previous studies on Ag_2O and Pt loaded WO_3 have proved that the surface noble metal (Ag or Pt) could work as effective multi-electron transfer active sites for oxygen reduction [21,23]. In the meantime, the photo-generated holes can oxidize the organic substrates. By this way, the $AgSbO_3–Ag–Ag_2O$ nanocomposite can remain stable during the following runs of the photocatalytic reactions. The schematic diagram showing the photocatalytic mechanism of pyrochlore $AgSbO_3$ during the photocatalytic reaction is shown in Scheme 1. A similar self-stable mechanism is previously reported over Ag-based photosensitive materials like Ag_2O and AgBr during the photocatalytic reactions [21,24]. However this is the first report that the Ag-containing multi-metal oxide can maintain its stability by partial formation of metallic Ag and Ag_2O in its surface.

4. Conclusion

In summary, nanocrystalline pyrochlore $AgSbO_3$ has been successfully synthesized by a facile hydrothermal method. The as-prepared $AgSbO_3$ shows a superior photocatalytic activity for the degradation of typical dye as compared to that prepared by the solid-state reaction. $AgSbO_3$ can maintain its structure stability and photocatalytic activity under visible light irradiations by partial formation of metallic Ag and Ag_2O on its surface during the photocatalytic degradation of organic pollutants. This study provides some new insights into the photocatalytic mechanism and the stability of Ag-based multi-metal oxide photocatalysts.

Acknowledgments

The work was supported by National Natural Science Foundation of China (20977016, U1033603), 973 program (2011CB612314), Program for Changjiang Scholars and Innovative Research Team in University (PCSIRT0818). The Award Program for Minjiang Scholar Professorship and the NSF of Fujian province for Distinguished Young Investigator Grant (2009J06004) to Z. Li are also acknowledged.

Appendix A. Supplementary data

Supplementary data associated with this article can be found, in the online version, at http://dx.doi.org/10.1016/j.apcatb.2012.04.033.

References

[1] M.R. Hoffmann, S.T. Martin, W. Choi, D.W. Bahnemann, Chemical Reviews 95 (1995) 69–96.
[2] A. Fujishima, T.N. Rao, D.A. Tryk, Journal of Photochemistry and Photobiology C 1 (2000) 1–21.
[3] C.C. Chen, W.H. Ma, J.C. Zhao, Chemical Society Reviews 39 (2010) 4206–4219.
[4] L. Zhang, W.Z. Wang, L. Zhou, M. Shang, S. Sun, Applied Catalysis B: Environmental 90 (2009) 458–462.
[5] Z.H. Ai, L.Z. Zhang, S.C. Lee, Journal of Physical Chemistry C 114 (2010) 18594–18600.
[6] Z. Bian, Y. Huo, Y. Zhang, J. Zhu, Y. Lu, H. Li, Applied Catalysis B: Environmental 91 (2009) 247–253.
[7] H.F. Shi, Z.S. Li, J.H. Kou, J.H. Ye, Z.G. Zou, Journal of Physical Chemistry C 115 (2011) 145–151.
[8] S. Zhu, T. Xu, H. Fu, J. Zhao, Y. Zhu, Environmental Science and Technology 41 (2007) 6234–6239.
[9] Z. Yi, J. Ye, N. Kikugawa, T. Kako, S. Ouyang, H. Stuart-Williams, H. Yang, J. Cao, W. Lou, Z. Li, Y. Liu, R.L. Withers, Nature Materials 9 (2010) 559–564.
[10] P. Wang, B.B. Huang, X.Y. Qin, X.Y. Zhang, Y. Dai, J.Y. Wei, M.H. Whangbo, Angewandte Chemie International Edition 47 (2008) 7931–7933.
[11] C. Hu, T.W. Peng, X.X. Hu, Y.L. Nie, X.F. Zhou, J.H. Qu, H. He, Journal of the American Chemical Society 132 (2010) 857–862.
[12] H. Kato, H. Kobayashi, A. Kudo, Journal of Physical Chemistry B 106 (2002) 12441–12447.
[13] R. Konta, H. Kato, H. Kobayashi, A. Kudo, Physical Chemistry Chemical Physics 5 (2003) 3061–3065.
[14] T. Kako, N. Kikugawa, J. Ye, Catalysis Today 131 (2008) 197–202.
[15] J. Singh, S. Uma, Journal of Physical Chemistry C 113 (2009) 12483–12488.
[16] H. Xue, Z.H. Li, L. Wu, Z.X. Ding, X.X. Wang, X.Z. Fu, Journal of Physical Chemistry C 112 (2008) 5850–5855.
[17] W.J. Liu, P.Y. Lin, H. Jin, H. Xue, Y.F. Zhang, Z.H. Li, Journal of Molecular Catalysis A: Chemical 349 (2011) 80–85.

[18] D. Muñoz-Rojas, G. Subías, J. Fraxedas, P. Gómez-Romero, N. Casañ-Pastor, Journal of Physical Chemistry B 109 (2005) 6193–6203.
[19] D. Muñoz-Rojas, G. Subías, J. Oró-Solé, J. Fraxedas, B. Martínez, M. Casas-Cabanas, J. Canales-Vázquez, J. Gonzalez-Calbet, E. García-González, R. Walton, N. Casañ-Pastor, Journal of Solid State Chemistry 179 (2006) 3883–3892.
[20] C.C. Chen, W.H. Ma, J.C. Zhao, Chemistry: A European Journal 10 (2004) 1956–1965.
[21] X.F. Wang, S.F. Li, H.G. Yu, J.G. Yu, S.W. Liu, Chemistry: A European Journal 17 (2011) 7777–7780.
[22] A.J. Bard, R. Parsons, J. Jordan, Standard Potentials in Aqueous Solution, Marcel Dekker, New York, 1985.
[23] R. Abe, H. Takami, N. Murakami, B. Ohtani, Journal of the American Chemical Society 130 (2008) 7780–7781.
[24] N. Kakuta, N. Goto, H. Ohkita, T. Mizushima, Journal of Physical Chemistry B 103 (1999) 5917–5919.